ENVIRONMENTAL RESEARCH
LETTERS

LETTER

Wildfire burn severity and emissions inventory: an example implementation over California

Qingqing Xu[1,*] ⓘ, Anthony LeRoy Westerling[1] ⓘ, Andrew Notohamiprodjo[1,2], Christine Wiedinmyer[3] ⓘ, Joshua J Picotte[4], Sean A Parks[5] ⓘ, Matthew D Hurteau[6], Miriam E Marlier[7] ⓘ, Crystal A Kolden[1], Jonathan A Sam[1] ⓘ, W Jonathan Baldwin[1] ⓘ and Christiana Ade[1]

1. Sierra Nevada Research Institute, University of California Merced, 5200 N. Lake Rd., Merced, CA 95340, United States of America
2. Spatial Informatics Group, 2529 Yolanda Ct., Pleasanton, CA 94566, United States of America
3. Cooperative Institute for Research in Environmental Sciences, University of Colorado Boulder, Boulder, CO 80309, United States of America
4. ASRC Federal Data Solutions, 7000 Muirkirk Meadows Drive Suite #100, Beltsville, MD, 20705, United States of America
5. Aldo Leopold Wilderness Research Institute, Rocky Mountain Research Station, USDA Forest Service, 790 East Beckwith Ave., Missoula, MT 59801, United States of America
6. Department of Biology, University of New Mexico, Albuquerque, NM 87131, United States of America
7. Department of Environmental Health Sciences, Fielding School of Public Health, University of California Los Angeles, Los Angeles, CA, United States of America
* Author to whom any correspondence should be addressed.

E-mail: qxu6@ucmerced.edu

Abstract

Wildfire severity is a key indicator of both direct ecosystem impacts and indirect emissions impacts that affect air quality, climate, and public health far beyond the spatial footprint of the flames. Comprehensive, accurate inventories of severity and emissions are essential for assessing these impacts and setting appropriate fire management and health care preparedness strategies, as is the ability to project emissions for future wildfires. The frequency of large wildfires and the magnitude of their impacts have increased in recent decades, fueling concerns about decreased air quality. To improve the availability of accurate fire severity and emissions estimates, we developed the wildfire burn severity and emissions inventory (WBSE). WBSE is a retrospective spatial burn severity and emissions inventory at 30 m resolution for event-based assessment and 500 m resolution for daily emissions calculation. We applied the WBSE framework to calculate burn severity and emissions for historically observed large wildfires (>404 hectares (ha)) that burned during 1984–2020 in the state of California, U.S., a substantially more extended period than existing inventories. We assigned the day of burning and daily emissions for each fire during 2002–2020. The framework described here can also be applied to estimate severity for smaller wildfires and can also be used to estimate emissions for fires simulated in California for future climate and land-use scenarios. The WBSE framework implemented in R and Google Earth Engine can provide quick estimates once a desired fire perimeter is available. The framework developed here could also easily be applied to other regions with user-modified vegetation, fuel data, and emission factors.

1. Introduction

Though some wildfires are essential to the Earth system and have beneficial effects on ecosystems that have evolved with fire, human influences have altered wildfire risk via increasing ignitions, climate change, and cumulative impacts of land management and use (Bowman *et al* 2009, Stephens *et al* 2013, Balch *et al* 2017, Abatzoglou *et al* 2018, McLauchlan *et al* 2020). In addition to ecosystem effects, wildfires directly impact people through property losses, injuries, mortality, and evacuations, while smoke and its health impacts are how the largest numbers of people are affected by wildfires through the regional transport of

smoke in the atmosphere (Finlay *et al* 2012, Reid *et al* 2016, Bowman *et al* 2017, Thomas *et al* 2017, Burke *et al* 2021).

The two most commonly used criteria for analyzing fire effects are burned area and burn severity (Key and Benson 2006, Kolden *et al* 2012, Meng and Zhao 2017). The degree to which a fire-disrupted ecosystem has changed is referred to as burn severity (Eidenshink *et al* 2007, Keeley and Syphard 2019). Because of differences in wind, topography, fuel conditions, and other factors, burned areas typically consist of complex landscape mosaics of low, moderate, and high burn severity (Turner *et al* 1994, Perry *et al* 2011, Birch *et al* 2015, Prichard *et al* 2020). Thus, landscape-scale quantification of burn severity is vital to identify the immediate and long-term influence on fire regimes, air quality, emissions, and other impacts. Passive spectral reflectance satellites and field observation have been used to determine burn severity. The change in Normalized Burn Ratio (NBR) between pre-and post-fire satellite images (dNBR) has become the primary index for remote sensing of severity. In the United States, the Monitoring Trends in Burn Severity Project (MTBS) (Eidenshink *et al* 2007), which is derived from long-running Landsat earth observing sensors, mapped burn severity for large fires dating back to 1984. However, the MTBS products have limitations, with sources of potential errors (e.g. subjective and not field validated severity classification thresholds) and a 2 year delay in including new fires in the database, that make the them less than ideal for research (Kolden *et al* 2015). The composite burn index (CBI) field method tabulates severity within 30 m plots by averaging measurements of several rating factors on a continuous scale ranging from 0.0 (unburned) to 3.0 (high severity) (Key and Benson 2006). On-the-ground burn severity was assessed following the CBI protocol only for 234 fires that burned in the contiguous United States (CONUS) during 1996–2018 (Picotte *et al* 2019).

Emission inventories are a critical input for a variety of modeling applications that seek to understand how emissions affect air quality, climate, and human health (Larkin *et al* 2014, Jaffe *et al* 2020, Pouliot *et al* 2020). Several global biomass burning emissions inventories have been produced and updated in recent decades. 'Bottom-up' inventories such as the Global Fire Emissions Database (GFED; van der Werf *et al* 2004, 2006, 2010, 2017) and the Fire INventory from NCAR (FINN; Wiedinmyer *et al* 2011), rely on satellite burned area and/or active fire detections, coupled with fuel loads, combustion completeness, and emissions factors to estimate fire emissions. GFED has provided monthly, daily, and three-hourly (since 2003) emissions data at 0.25 degrees since 1997. FINN has provided daily estimates at 1 km resolution since 2002. 'Top-down' inventories such as the Global Fire Assimilation System (GFAS; Kaiser *et al* 2011), Quick Fire Emissions Database (QFED; Darmenov

and da Silva 2015), and Fire Energetics and Emissions Research (FEER; Ichoku and Ellison 2014) rely on fire radiative power observations to compute emissions, along with different approaches to address cloud cover and to compute scaling factors for fire emissions. GFAS, QFED and FEER produce daily estimates at 0.1 degrees since 2003, 2000, and 2003, respectively. Several emission inventories for the CONUS are currently available. The United States Environmental Protection Agency National Emissions Inventory (US EPA NEI, Raffuse *et al* 2012) estimates emissions from all sources including wildfire and prescribed fire emissions every 3 years. The Wildland Fire Emissions Information System (WFEIS) (French *et al* 2014) provides tools for assessing wildland fire emissions in area-of-interest or for an identified fire event. It also provides pre-calculated emissions data on state or country level on monthly/yearly scale with the earliest records back to 1984. Comparisons of fire emissions inventories have revealed variability in inventory results, with each having advantages and disadvantages (Larkin *et al* 2014, Faulstich *et al* 2022). Despite all efforts, there is an urgent need for burn severity and emissions inventories at the scale of actionable management (e.g. fuel reduction treatments) and over longer temporal periods.

Here, we introduce the WBSE and present a detailed description of the inventory model, initial results using California historical large wildfires as an example, comparison with other inventory estimates, and a discussion of uncertainties. The primary objective of this manuscript is to describe the model, and our comparison with other emissions inventories is limited in scope. Similarly, the historical reconstructions of wildfire severity maps and emissions are analyzed in more detail in a companion paper. This study benefits from the recently available regression models developed at national and regional scales transforming the dNBR/NBR to CBI to consistently map burn severity in a transparent manner (Picotte *et al* 2021). Following Wiedinmyer *et al* (2011), we use modified algorithms and updated fuel emissions and consumption factors drawing on recently published field and remote sensing data to better capture emissions from more extreme fires. Larger, severe wildfires in California increasingly impact ecosystems, human health and life, communities, and infrastructure due to expanding wildland-urban interfaces, fuel accumulation from a century of fire exclusion policies, and increasing aridity, which increases the amount of biomass available to burn. (Abatzoglou and Williams 2016, Westerling 2016, Williams *et al* 2019, Goss *et al* 2020, Goodwin *et al* 2021). The comprehensive, long-term event and daily emissions records described here could be used to study health effects of wildfire smoke, either by combining them with transport modeling to model air quality and estimate exposures, or by incorporating them into statistical models predicting health impacts as a direct

function of estimated emissions. These data will also facilitate analyses of changing emissions impacts on the carbon cycle over the last three decades. High resolution severity and emissions raster maps are generated for each fire event to support further spatial analysis. While the emissions calculated for California with WBSE are not a substitute for real-time daily emissions estimates, it is designed to extend the estimated emissions record back to 1984 with a finer spatial resolution and provide more up-to-date estimates on emissions factors reflecting information from California's recent extreme fires.

2. Methods

The WBSE provides estimates of 30 m resolution burn severity, and emissions of CO_2, CO, CH_4, non-methane organic compounds (NMOC), SO_2, NH_3, NO, NO_2, nitrogen oxides ($NO_x = NO + NO_2$), $PM_{2.5}$, OC, and BC. We implemented WBSE for California large wildfires on a per-fire event scale since 1984 and also a daily scale since 2002. The inventory implementation steps, input datasets, and output data are summarized in figure 1. Emissions of all species are calculated as a function of area burned, fuel loading, the fraction of vegetation burned based on burn severity, and an emissions factor specific to each vegetation type using the following equation modified from the FINN model (Wiedinmyer *et al* 2011):

$$E_i = A_{v,s} \times F_v \times cr_{v,s} \times ef_{v,i} \qquad (1)$$

Where E_i is the mass of emission species *i* emitted, $A_{v,s}$ and $cr_{v,s}$ are the area burned and fuel consumption rate of general vegetation class *v* (grass, shrub, forest <5500 ft, forest 5500–7500 ft, forest >7500 ft) under severity class *s* (low, moderate, and high severity), F_v is the fuel loading of vegetation class *v*, and $ef_{v,i}$ is the emission factor of emission species *i* for vegetation *v*.

The FINN model was developed to estimate global emissions from open burning at 1 km resolution. It has been used in various modeling studies for modeling atmospheric chemistry and air quality (Jiang *et al* 2012, Val Martin *et al* 2013, Brey *et al* 2018). The primary differences of emission calculation methods between WBSE and FINN are that WBSE calculates emissions per fire event while FINN provides global emission estimates in real time. Other differences include (a) obtaining the area burned by fire severity class from a new CBI-based burned area product (based on fire perimeters published by MTBS and California Department of Forestry and Fire Protection (CAL FIRE)) while the Moderate Resolution Imaging Spectroradiometer (MODIS) Thermal Anomalies Product is used in FINN; (b) assigning vegetation type from the LANDFIRE existing vegetation type (EVT) product to general vegetation classes with an updated crosswalk from Hurteau *et al* (2014)

while the MODIS land cover product is used in FINN; (c) calculating fuel loading and consumption based on burn severity for each vegetation class while fuel consumption is based on a function of tree cover and fuel loading for generic land cover classifications for the global regions in FINN; (d) Using region specific emissions factors for California and Western U.S. ecosystems to calculate emissions for the example implementation over California; and (e) assigning the day of burning based on MODIS and VIIRS data for each large wildfire burned since 2002. The inventory has a spatial resolution of 30 m for per-fire emission estimates and 500 m for daily emissions rather than the 1 km resolution in FINN. The area burned in low, moderate, and high burn severity is calculated from Landsat-derived indices (NBR and dNBR) using a hierarchy of regression models developed by Picotte *et al* (2021). We recognize that other fire severity metrics have been developed (e.g. RdNBR and RBR; Miller and Thode 2007 & Parks *et al* 2014, respectively), but we opted to use NBR/dNBR because of the regionally specific models developed by Picotte *et al* (2021) that used NBR/dNBR. We do not have a quantitative assessment of the uncertainty; however, we assign a factor of 2 to the uncertainty due to all of the inputs to the model following Wiedinmyer *et al* (2011). A matrix table of 30 m pixel level $PM_{2.5}$ emission uncertainty for five general vegetation classes due to burn severity classification error is given in supplementary table 3.

Fire records for California from 1984 to 2019 were retrieved from MTBS (https://mtbs.gov/viewer/index.html) via interactive viewer on 8 May 2021, resulting in a dataset with a total of 1623 wildfires. We also acquired fire perimeters for 74 large wildfires in 2020 from CAL FIRE (https://frap.fire.ca.gov/frap-projects/fire-perimeters/) and calculated dNBR for each 2020 fire using the dNBR calculation tool with Google Earth Engine (GEE) (figure 2). This process first selects either initial assessment or extended assessment for each fire. The initial assessment utilizes Landsat images acquired immediately after a fire to capture first-order fire effects. The extended assessment uses images obtained during the growing season following the fire to identify delayed first-order effects and dominant second-order effects (Eidenshink *et al* 2007). We utilized LANDFIRE Biophysical Settings (BPS) to determine which assessment type to apply for each fire burned in 2020. After Picotte *et al* (2021), we used extended assessment if the majority of general vegetation groups within the fire perimeter are forests, while initial assessment is used when the majority of general vegetation groups are grassland/shrubland. By contrast, MTBS uses extended assessment for forest and shrubland types. We did not delineate grasslands into burn severity categories. Instead, we classified them as burned ('grass burn') because of difficulties in assessing vegetation change. Post-fire images for extended assessment

Figure 1. Diagram of Wildfire Burn Severity and Emissions Inventory (WBSE) inventory steps and datasets.
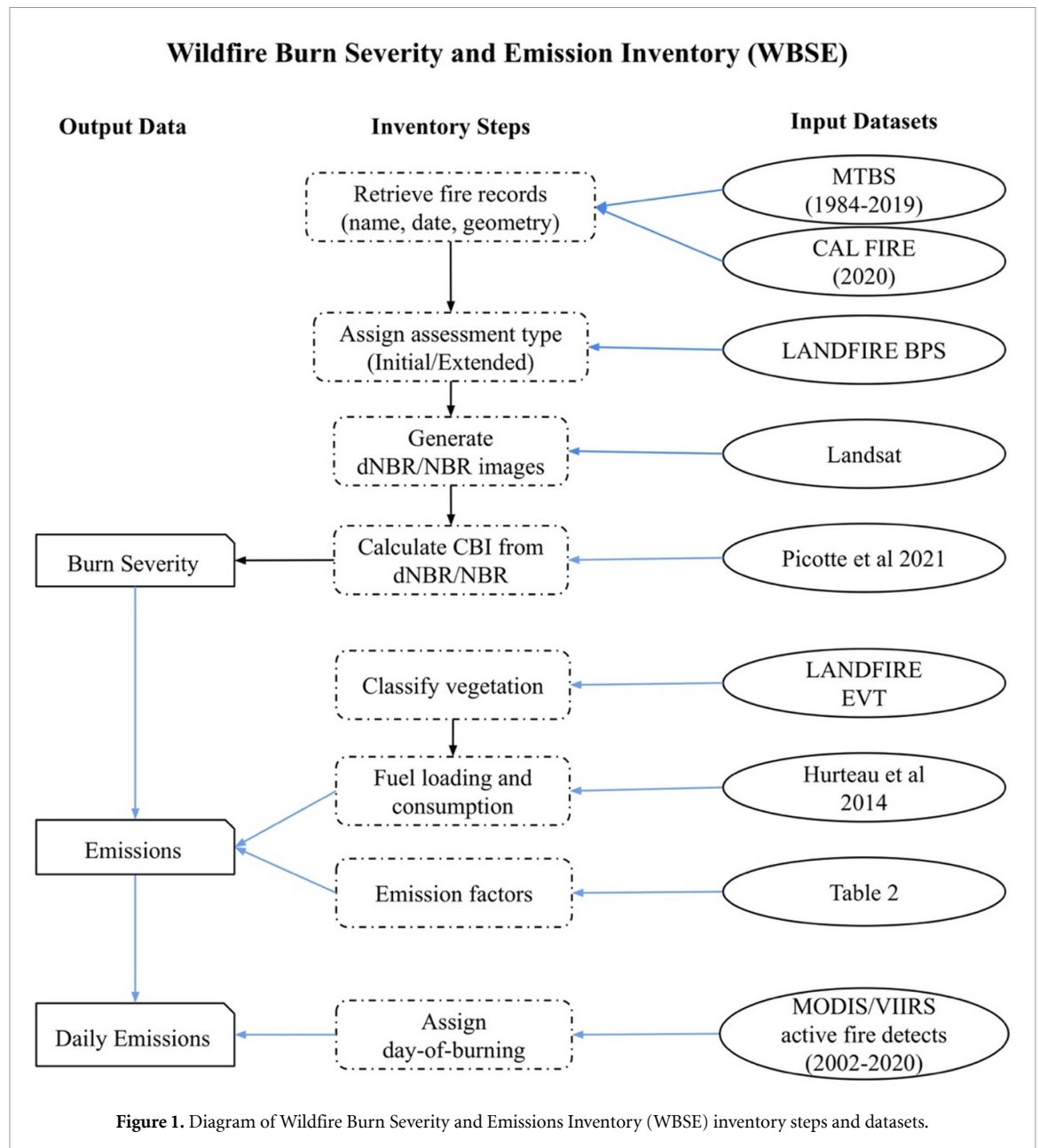
were selected during the next peak of the green season (June–September) using the mean compositing approach suggested by Parks *et al* (2018). Composite post-fire images acquired immediately within two months after the fire containment dates were used for the initial assessment. Composite pre-fire images for extended and initial assessments were acquired with the matching periods from the preceding year. The dNBR images were produced by quantifying the spectral difference between composite pre-fire and post-fire Landsat scenes.

Burn severity for a given fire can have either a linear or non-linear relationship to dNBR/NBR (Picotte *et al* 2021). So to make an equivalent burn severity product across all fires, we calculated the unitless, continuous CBI variable from dNBR/NBR values using the linear and Sigmoid B regression models developed for the CONUS by Picotte *et al*

(2021). We first applied the MTBS or CAL FIRE perimeter shapefile for each wildfire event to crop the BPS raster file. The BPS data are categorized into one of 12 vegetation groups. For CBI calculations, we further grouped 'Conifer', 'Hardwood', 'Hardwood-Conifer', 'Shrubland', and 'Riparian' into the 'forest/shrub' classification; 'Savanna', 'Sparse', and 'Grassland' into the 'grass' classification; and the rest 'Barren-Rock/Sand/Clay', 'Open Water', and 'Perennial Ice/Snow' into the 'unchanged' group. We applied the decision tree framework (figure 3) for each pixel categorized as forest/shrub to convert the dNBR/NBR value into a CBI value. CBI values less than or equal to 0 were arbitrarily assigned a value of 0.001 to be classified into the 'unburned' group. Modeled CBI values larger than 3 were assigned the value 3 to be classified into the 'high severity' group. For the grass group, we set a CBI value of 3.5 to
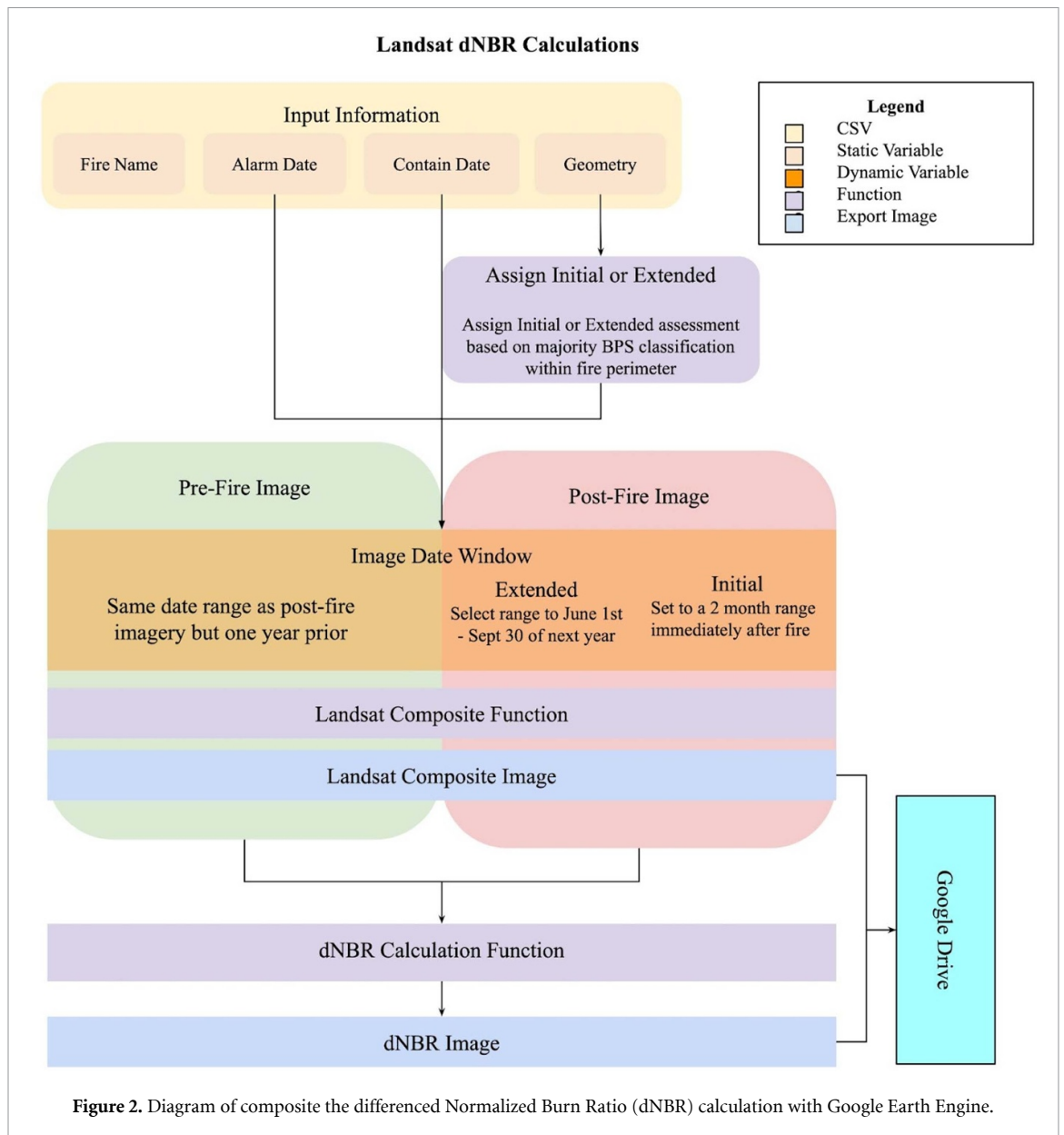
Figure 2. Diagram of composite the differenced Normalized Burn Ratio (dNBR) calculation with Google Earth Engine.
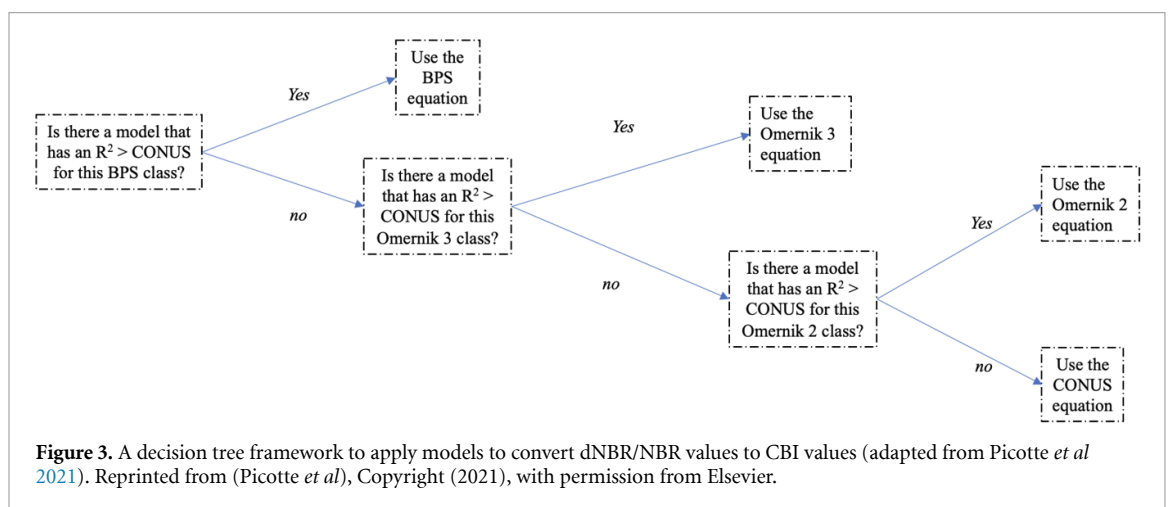

Figure 3. A decision tree framework to apply models to convert dNBR/NBR values to CBI values (adapted from Picotte *et al* 2021). Reprinted from (Picotte *et al*), Copyright (2021), with permission from Elsevier.

indicate that this pixel was a grass burn. CBI values were then classified following thresholds modified based on Crotteau *et al* (2014) into six severity classes: unburned, low severity, moderate severity, high severity, grass burn, and non-processing area.

Fuel categories were assigned from LANDFIRE EVT products. EVT represents the current distribution of the terrestrial ecological systems classification (Rollins 2009), and the vegetation layers were updated every couple of years to account for landscape disturbances. The most appropriate version was applied for each fire event depending on the burn year—EVT data version LF 1.0.5, 1.2.0, 1.3.0, 1.4.0, 2.0.0 were applied to wildfires burned before the year of 2002, 2002–2010, 2011–2012, 2013–2014, and after 2014, respectively. For emissions calculations, EVT data were then categorized into five general vegetation categories: grass, shrub, forest under 5500 feet (1676 m), forest between 5500–7500 feet (1676–2286 m), and forest above 7500 feet (2286 m), updated for California ecosystems (supplementary table 1). Fuel consumption was determined following Hurteau *et al* (2014) assigning fuel loading and consumption values for each severity class for the five general vegetation categories based on the First Order Fire Effects Model v5 (Reinhardt *et al* 1997) (supplementary table 2).

The LF EVT classes were assigned to generic vegetation classes of FINN so that emission factors could be applied. Emission factors for greenhouse gases, particulate matter, and reactive trace gases were updated with recent data for each general vegetation class using results from recent field campaigns and studies specific for California ecosystems and Western U.S. ecosystems (see table 1).

To assign the day of burning for individual pixels, NASA fire information for resource management system (FIRMS) active fire products from MODIS (Collection 6) within 750 m of the fire perimeter shapefiles supplied by MTBS or CAL FIRE were selected for interpolation to account for detections that might be outside the boundary due to detection radius. VIIRS 375 m data, when available since 2012, was added to complement MODIS data with improved performance to assign burn dates using the fire progression raster tool (figure 4). We filtered the MODIS/VIIRS detection points to the date range of interest and created a 500 m buffer around each point. Points were then converted to circle polygons to represent each point's detection extent properly. The average date was selected as the proper date in regions of overlapping buffers. We then calculated daily emissions and assigned them to the centroids of the aggregated daily progression polygons. Versions were also implemented using the earliest or latest date of detection points to assign the day of burning (results not reported here, but maps are available).

3. Results and discussion

Burn severity and emissions were calculated for 1697 large wildfire events in California during 1984–2020 at a 30 m resolution scale using the WBSE framework described above. Day of burning and daily

Table 1. Emission factors (g species emitted per kg biomass burned) assigned to Grasslands, Shrublands, and Forests.

Emission factors	Temperate forest	Shrublands	Grasslands
CO_2	1650[a]	1588[b]	1421[h]
CO	80[a]	97[b]	56[h]
CH_4	3.7[a]	2.2[b]	2.9[h]
NMOC	24[c]	24[d]	28[e]
SO_2	0.94[a]	0.73[b]	3.0[h]
NH_3	1.17[f]	1.68[g]	0.56[h]
NO	0.90[f]	1.3[g]	2.9[h]
NO_2	0.99[f]	0.94[g]	3.1[h]
NO_x (as NO)	1.2[f]	2.1[g]	3.9[i]
$PM_{2.5}$	10.6[a]	7.9[a]	7.2[i]
OC	11.6[j]	3.7[k]	2.6[k]
BC	0.4[j]	1.31[k]	0.37[k]

[a] Average of Forest emission factors, table 5, Prichard *et al* (2020).
[b] Shrublands and Grasslands emissions factors, table 5, Prichard *et al* (2020).
[c] Average NMOC emissions for forest fires from Permar *et al* (2021).
[d] Average NMOC emissions from sagebrush fires from Permar *et al* (2021).
[e] Sum of NMOCs in Akagi *et al* (2011), updated February 2015 for Savanna.
[f] Average of Forest emission factors, table 5, Prichard *et al* (2020) and forest fire E.F.s from Lindaas *et al* (2020).
[g] Average of Shrubland emission factors, table 5, Prichard *et al* (2020) and sagebrush fire E.F.s from Lindaas *et al* (2020).
[h] Grassland emission factors, table 5, Prichard *et al* (2020).
[i] Akagi *et al* (2011), updated February 2015 for Savanna.
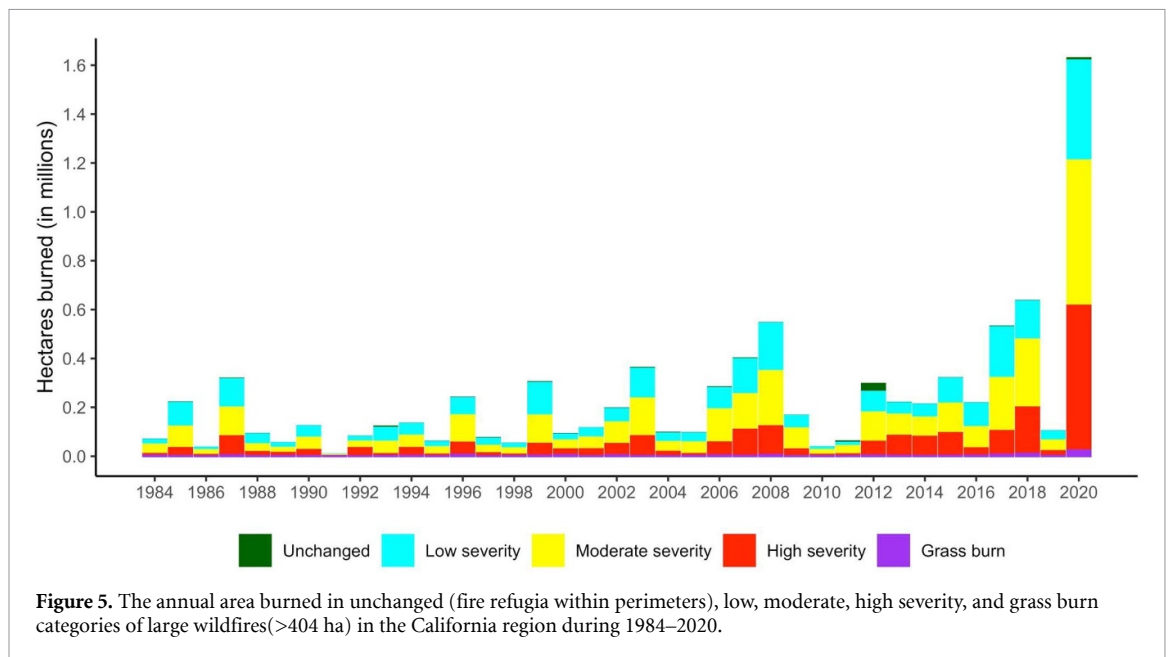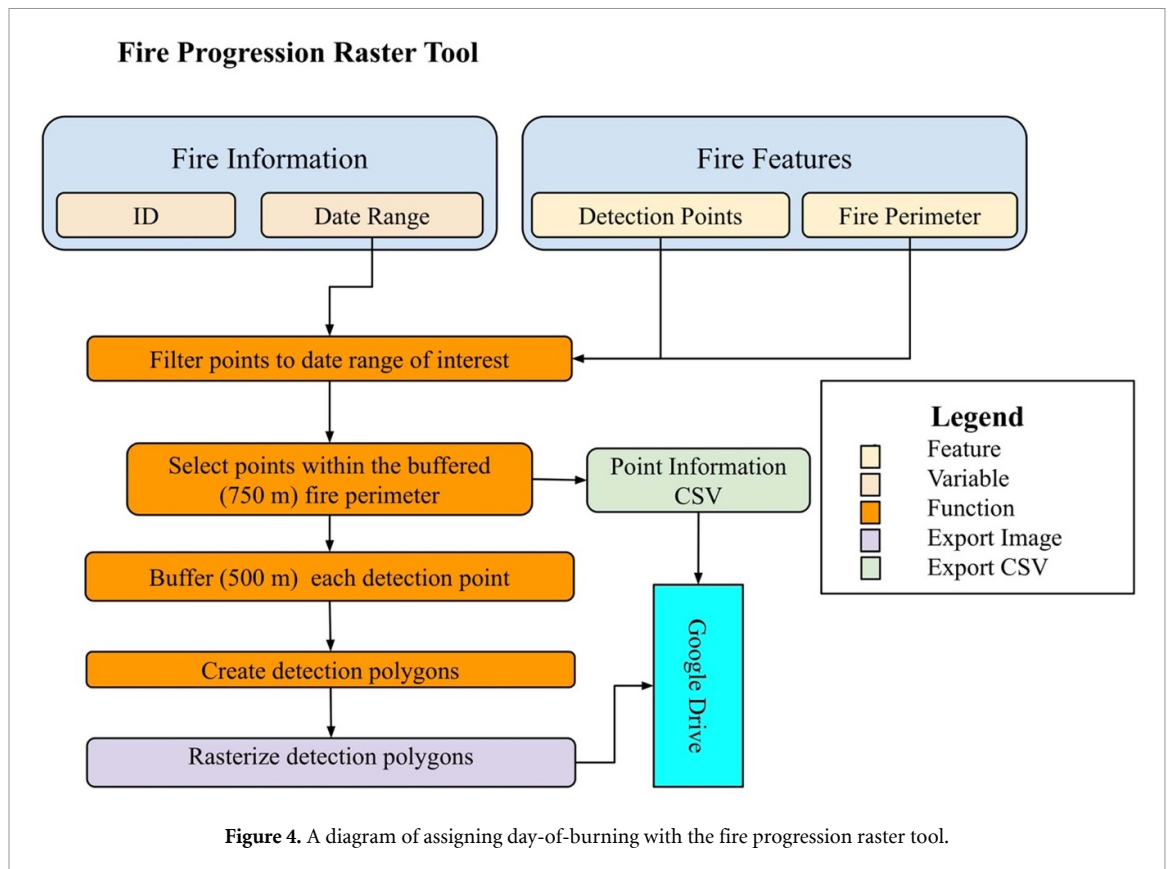[j] Supplemental table 2, Permar *et al* (2021).
[k] Wiedinmyer *et al* (2011).

emissions were calculated for each fire during 2002–2020. Data processing and calculations were implemented using R (R Core Team 2021) and GEE (Gorelick *et al* 2017). The datasets are available for download and use.

3.1. Burn severities

Over the 1984–2020 period, the average annual area burned (excluding obscured area) was 0.23 million ha with substantial interannual variability (figure 5). Obscured area includes data gaps associated with clouds, smoke, or the Landsat 7 ETM+ scan-line corrector failure (Key 2006), affecting 0.3% of the area mapped within historical burn perimeters. The maximum annual area burned was 1.6 million ha in 2020, about 220 times the area burned in the minimum year of 1991. Of the approximately 8.5 million ha mapped by this project, about 63% burned at moderate or high severity (figure 6).

As MTBS has been previously established as a rough estimate of burn severity rather than a rigorous calculation for a specified need (e.g. emissions calculations), a direct comparison of the total area burned by severity category between MTBS and WBSE is helpful to contextualize the more rigorous approach applied here. MTBS analysts subjectively classify NBR and dNBR into six classes (unburned to low,

Figure 4. A diagram of assigning day-of-burning with the fire progression raster tool.

Figure 5. The annual area burned in unchanged (fire refugia within perimeters), low, moderate, high severity, and grass burn categories of large wildfires(>404 ha) in the California region during 1984–2020.

low, moderate, high, increased greenness, and non-processing area mask) (Kolden *et al* 2015). Here, we empirically classified modeled CBI values into four classes (unchanged, low, moderate, and high) and two categories of 'grass burn' and 'non-processing area' using an objective, standardized procedure. A pixel-level classification comparison (excluding non-processing area) indicates that ∼45% of the pixels in both datasets were classified as the same burn severity (cells highlighted in blue in table 2); however, WBSE

burn severity was generally higher than MTBS (cells highlighted in pink in table 3). We found that 22% percent of pixels classified as low burn severity by MTBS were classified as moderate burn severity by WBSE. By contrast, less than 2% of pixels were classified as having higher burn severity by MTBS than WBSE (cells highlighted in green in table 3). The remaining pixels were mainly classified as low burn severity by WBSE but unburned to low burn severity by MTBS.
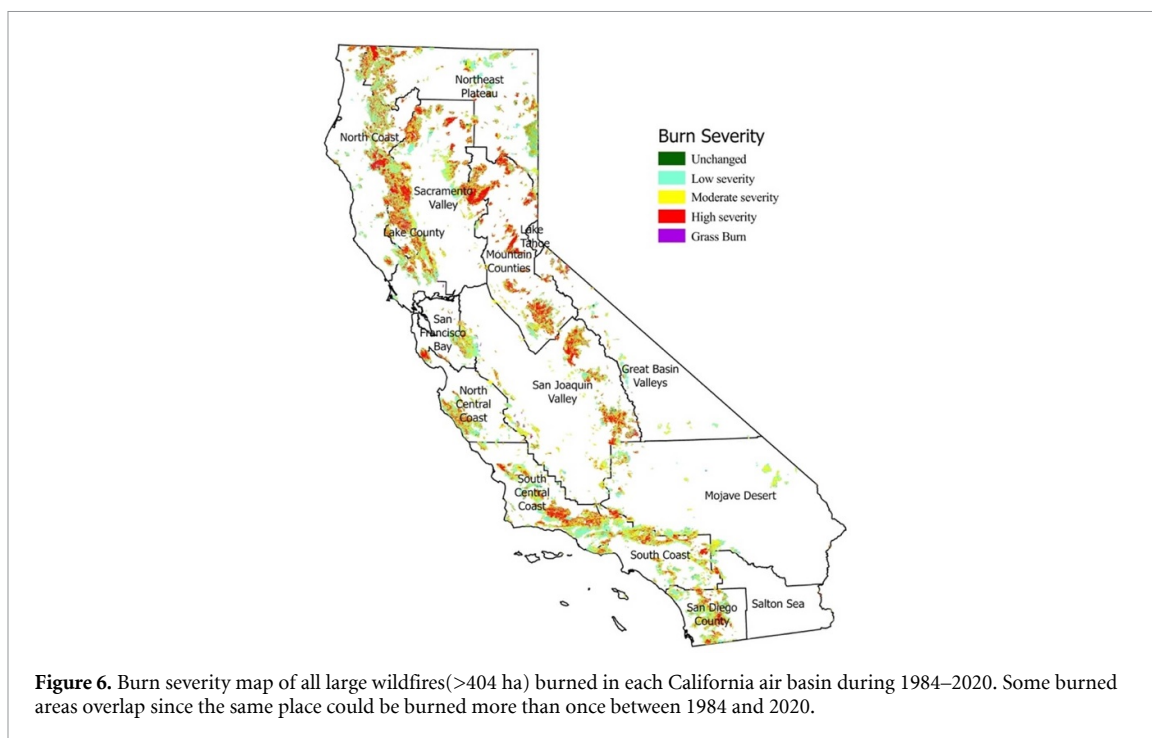
Figure 6. Burn severity map of all large wildfires(>404 ha) burned in each California air basin during 1984–2020. Some burned areas overlap since the same place could be burned more than once between 1984 and 2020.

Table 2. Pixel level burn severity classification comparison of MTBS and WBSE (unit: %).

MTBS \ WBSE	Unchanged	Low	Moderate	High	Grass burn	Total
Unburned to low	<1	19	<1	<1	<1	21
Low	<1	14	22	<1	<1	37
Moderate	<1	<1	17	8	<1	25
High	<1	<1	2	14	<1	16
Increased greenness	<1	<1	<1	<1	<1	1
Total	1	34	42	22	1	100

Blue: same burn severity classification in MTBS and WBSE.

Pink: higher severity classification in WBSE.

Green: lower severity classification in WBSE.

White: class not comparable between products.

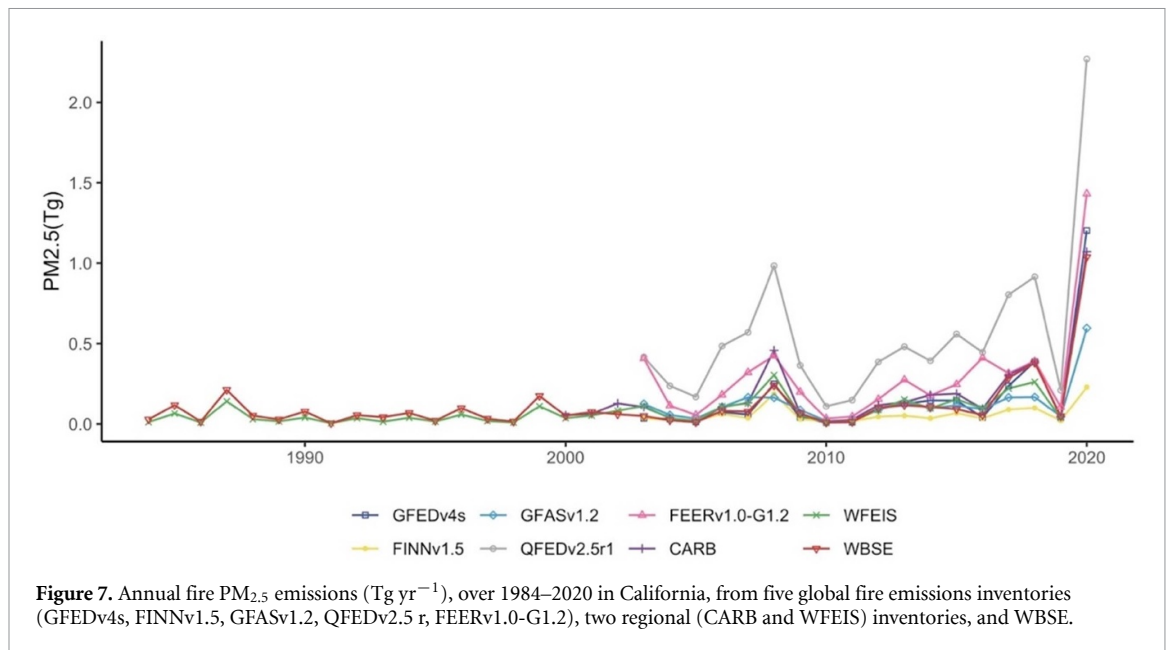**Table 3.** Summary statistics of emissions during 1984–2020.

	Min (t)[a]	Median (Gg)[a]	Mean (Gg)[a]	Max (Gg)[a]	Annual average (Gg)[b]
CO_2	8.185	73.59	388.519	48 154	17 819
CO	0.323	3.856	19.834	2397	910
CH_4	0.017	0.137	0.798	104	37
NMOC	0.161	1.103	5.734	704	263
SO_2	0.017	0.043	0.222	27	10
NH_3	0.003	0.06	0.303	36	14
NO	0.017	0.05	0.245	28	11
NO_2	0.018	0.048	0.243	29	11
NO_x	0.022	0.072	0.346	38	16
$PM_{2.5}$	0.041	0.426	2.365	302	108
OC	0.015	0.355	2.302	315	106
BC	0.002	0.032	0.143	15	7

[a] Min, median, mean, and max is the value in the context of each fire event.

[b] Annual average is the amount averaged over the 1984–2020 period.

t: metric tons.

Gg: Gigagrams.

Figure 7. Annual fire PM$_{2.5}$ emissions (Tg yr^{-1}), over 1984–2020 in California, from five global fire emissions inventories (GFEDv4s, FINNv1.5, GFASv1.2, QFEDv2.5 r, FEERv1.0-G1.2), two regional (CARB and WFEIS) inventories, and WBSE.

3.2. Emissions estimates

Summary statistics of trace gases and particulate species emitted by wildfires in California during 1984–2020 are shown in table 3. The annual average of CO$_2$ and PM$_{2.5}$ emitted are 18 Tg and 108 Gg, respectively, with a significant interannual variation. Emissions from wildfires varied significantly and depended on fire size, fire severity, and vegetation characteristics. The largest wildfire was the 2020 August Complex, which burned 417 898 ha in six counties in the Coast Range of Northern California and produced the maximum amount of all types of emissions. This single fire emitted approximately 2.5 times the annual average wildfire emissions for all of California for the past 37 years.

We compared our emissions estimates of PM$_{2.5}$ to five global fire emissions inventories (GFEDv4s, FINNv1.5, GFASv1.2, QFEDv2.5r, FEERv1.0-G1.2) that are commonly used in atmospheric modeling simulations by extracting monthly and annual emissions for California from 2003 to 2020 using the FIRECAM online tool (Liu *et al* 2020). We note that GFEDv4s values assessed here for 2017–2020 emissions are preliminary. Annual emissions were also extracted from California Air Resource Board (CARB 2021) for 2000–2020 and WFEIS for 1984–2020. The estimates agree reasonably well with other emissions inventories, although they may vary by as much as a factor of 3 annually across inventories (figure 7).
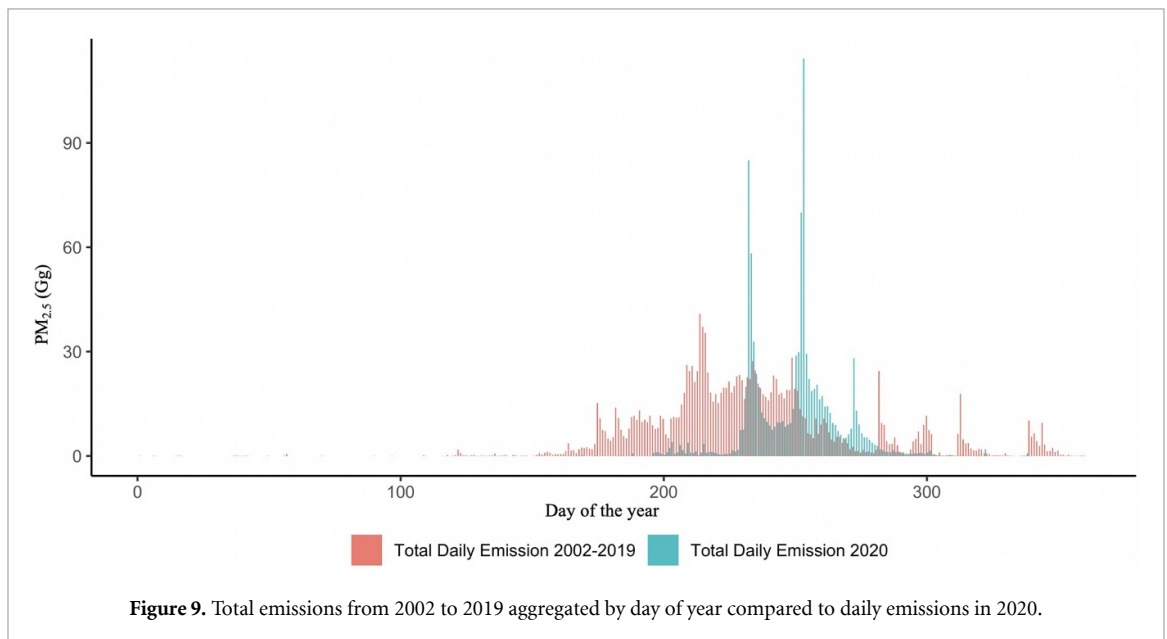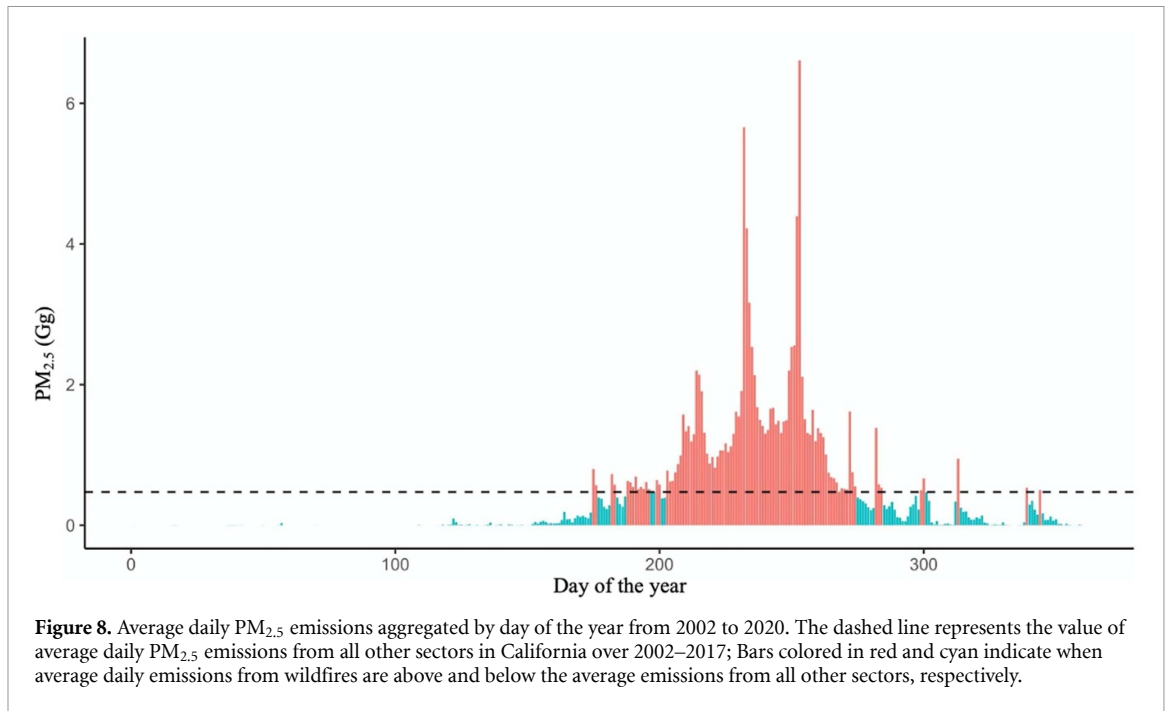
3.3. Daily emissions

We calculated daily emissions for a total of 841 fires since 2002 when MODIS data were available. For 2002–2020, 6% percent of the original FIRMS fire points were removed annually due to low detection confidence. Seventy-four fire events were removed from the daily emissions database due to less than

ten MODIS/VIIRS fire detections falling within the WBSE fire perimeter; the daily emissions from these events are considered uncertain given the low number of fire detections (after Parks 2014). These 74 fires were also small fire events, and their total emissions only accounted for less than 1% of the emissions during 2002–2020. The average daily emissions over the summer during 2002–2020 are higher compared to the average amount (0.47 Gg[8]) of daily PM$_{2.5}$ emissions from all other sectors in California over 2002–2017 (figure 8). The extremes that peak around the middle of August and September are primarily contributed by the 2020 wildfires (figure 9).

3.4. Limitations and uncertainties

The results of this research should be considered with some limitations in mind, as uncertainties are associated with several aspects of the calculation process. Uncertainties related to the FINN model, including fire location, timing and area burned, vegetation identification, fuel loading, and fuel consumption, and emission factors, are described in detail by Wiedinmyer *et al* (2011). The modified FINN model used here reduces uncertainties related to fire numbers and sizes by using documented fire records rather than satellite detections. However, fire perimeters used in this calculation for wildfires during 1984–2019 were generated by on-screen interpretation and delineation of dNBR images by MTBS analysts. We used MTBS perimeters to better compare the burn severity difference between WBSE and MTBS. The results may change slightly when using other documented fire perimeter data; for example, we also calculated emissions since 1984 using perimeters from

---

[8] Calculated based on air pollutant emissions trends data from the United States Environmental Protection Agency www.epa.gov/air-emissions-inventories/air-pollutant-emissions-trends-data.

Figure 8. Average daily $PM_{2.5}$ emissions aggregated by day of the year from 2002 to 2020. The dashed line represents the value of average daily $PM_{2.5}$ emissions from all other sectors in California over 2002–2017; Bars colored in red and cyan indicate when average daily emissions from wildfires are above and below the average emissions from all other sectors, respectively.

Figure 9. Total emissions from 2002 to 2019 aggregated by day of year compared to daily emissions in 2020.

CAL FIRE (not shown here but available). Uncertainty also arises from misidentification of land cover: (a) the burn severity classification is based on the LF BPS dataset, which characterizes vegetation systems that may have been dominant on the landscape before Euro-American settlement, but may not be representative of current vegetation; (b) fuel loading is calculated based on LF EVT, which represents the current distribution of the terrestrial ecological systems classification, but this dataset is infrequently updated and may not accurately represent the conditions at the time of burning. Fuel loading, consumption, and emission rates were constant values for general vegetation categories and severity classes, which may not reproduce the full heterogeneity of land cover. The

day of burning was assigned with an average date in regions of overlapping buffers in this analysis, and the results change slightly if the earliest date or latest date is used as the proper date. In addition, around 5% of emissions were not assigned to a valid date since no fire points were detected by satellites. This may lead to a slight underestimate of daily emissions and thus the derived impact on air quality and public health. The open-source, open data framework presented here can be further refined as needed to address any of these limitations. Likewise, Picotte *et al* (2021) 's severity algorithms implemented here are designed to be robust to limitations in the available plot-level CBI data and can be extended to incorporate new plot-level data as they become available.

4. Conclusions

The WBSE framework implemented in R and GEE produces quick estimates of burn severity and emissions from wildfires at a 30 m spatial resolution and day of burning and daily emissions at 500 m spatial resolution. The burn severity estimates have advantages over MTBS products in that: (a) burn severity is categorized consistently based on field-validated equations, rather than subjective thresholds for each fire event; (b) an initial assessment can be estimated as soon as the desired fire perimeter is available; (c) they enable consistent annual estimates for wildfires burned in California during 1984–2020, which facilitates objectively quantifying changes over time and across fires. Further, daily emissions estimates can be calculated for periods when daily fire activity data are available (beginning in 2002). The daily emission estimates are currently being incorporated into chemical transport models to evaluate the impact of wildfire smoke on downwind air quality and population exposure. This work facilitates climate vulnerability assessments that include the effects of smoke on public health and provides estimates of greenhouse gas emissions during a fire. The publicly available WBSE fire severity history and emissions inventory offers a valuable, open-source resource for the fire research community, readily updated after each fire season, with a framework that allows for iterative improvements as more data become available. Future planned improvements include automated fire perimeter mapping of observed fires and incorporating interactive web tools to enable users to estimate fire emissions for simulated fire severity maps with user-modified climate and fuels management. For California's Fifth State Climate Assessment, the Pyregence Consortium is simulating individual wildfire events (location, date, size, and severity fraction) for future climate, land use and fuels management scenarios, mapping simulated severity at 30 m across the state, and using the framework presented here for estimating emissions from individual large fire simulations through 2100.

Data availability statement

Acknowledgments

Code availability

ORCID iDs

Qingqing Xu ● https://orcid.org/0000-0001-9532-8815
Anthony LeRoy Westerling ●
https://orcid.org/0000-0003-4573-0595
Christine Wiedinmyer ● https://orcid.org/0000-0001-9738-6592
Sean A Parks ● https://orcid.org/0000-0002-2982-5255
Miriam E Marlier ● https://orcid.org/0000-0001-9333-8411
Jonathan A Sam ● https://orcid.org/0000-0002-7208-6224
W Jonathan Baldwin ● https://orcid.org/0000-0001-5470-6306

References

Abatzoglou J T and Williams A P 2016 Impact of anthropogenic climate change on wildfire across Western US forests *Proc. Natl Acad. Sci.* **113** 11770–5

Abatzoglou J T, Williams A P and Barbero R 2018 Global emergence of anthropogenic climate change in fire weather indices *Geophys. Res. Lett.* **46** 326–36

Akagi S K, Yokelson R J, Wiedinmyer C, Alvarado M J, Reid J S, Karl T, Crounse J D and Wennberg P O 2011 Emission factors for open and domestic biomass burning for use in atmospheric models *Atmos. Chem. Phys.* **11** 4039–72

Balch J K, Bradley B A, Abatzoglou J T, Nagy R C, Fusco E J and Mahood A L 2017 Human-started wildfires expand the fire niche across the United States *Proc. Natl Acad. Sci.* **114** 2946–51

Birch D S, Morgan P, Kolden C A, Abatzoglou J T, Dillon G K, Hudak A T and Smith A M S 2015 Vegetation, topography and daily weather influenced burn severity in central Idaho and western Montana forests *Ecosphere* **6** 1–23

Bowman D M J S *et al* 2009 Fire in the Earth system *Science* **324** 481–4

Bowman D M J S, Williamson G J, Abatzoglou J T, Kolden C A, Cochrane M A and Smith A M S 2017 Human exposure and sensitivity to globally extreme wildfire events *Nat. Ecol. Evol.* **1** 0058

Brey S J, Barnes E A, Pierce J R, Wiedinmyer C and Fischer E V 2018 Environmental conditions, ignition type, and air quality impacts of wildfires in the southeastern and Western United States *Earth's Future* **6** 1442–56

Burke M, Driscoll A, Heft-Neal S, Xue J, Burney J and Wara M 2021 The changing risk and burden of wildfire in the United States *Proc. Natl Acad. Sci.* **118** e2011048118

California Air Resource Board 2021 Wildfire emissions & burned area estimates 2000–2020 (available at: https://ww2.arb.ca. gov/sites/default/files/2021-07/Wildfire%20Emission%20 Estimates%20for%202020%20_Final.pdf) (Accessed 12 December 2021)

Crotteau J S, Ritchie M W and Varner J M 2014 A mixed-effects heterogeneous negative binomial model for postfire conifer regeneration in Northeastern California, USA *For. Sci.* **60** 275–87

Darmenov A S and da Silva A M 2015 *The Quick Fire Emissions Dataset (QFED): Documentation of Versions 2.1, 2.2 and 2.4* (*Technical Report Series on Global Modeling and Data Assimilation* vol 38) ed R D Koster (Greenbelt, MD: National Aeronautics and Space Administration) p 201

Eidenshink J, Schwind B, Brewer K, Zhu Z-L, Quayle B and Howard S 2007 A project for monitoring trends in burn severity *Fire Ecol.* **3** 3–21

Faulstich S D, Schissler A G, Strickland M J and Holmes H A 2022 Statistical comparison and assessment of four fire emissions inventories for 2013 and a large wildfire in the Western United States *Fire* **5** 27

Finlay S E, Moffat A, Gazzard R, Baker D and Murray V 2012 Health impacts of wildfires *PLoS Curr.* **4** e4f959951cce2c

French N H F *et al* 2014 Modeling regional-scale wildland fire emissions with the wildland fire emissions information system *Earth Interact.* **18** 1–26

Goodwin M J, Zald H S J, North M P and Hurteau M D 2021 Climate-driven tree mortality and fuel aridity increase wildfire's potential heat flux *Geophys. Res. Lett.* **48** e2021GL094954

Gorelick N, Hancher M, Dixon M, Ilyushchenko S, Thau D and Moore R 2017 Google earth engine: planetary-scale geospatial analysis for everyone *Remote Sens. Environ.* **202** 18–27

Goss M, Swain D L, Abatzoglou J T, Sarhadi A, Kolden C A, Williams A P and Diffenbaugh N S 2020 Climate change is increasing the likelihood of extreme autumn wildfire conditions across California *Environ. Res. Lett.* **15** 094016

Hurteau M D, Westerling A L, Wiedinmyer C and Bryant B P 2014 Projected effects of climate and development on California wildfire emissions through 2100 *Environ. Sci. Technol.* **48** 2298–304

Ichoku C and Ellison L 2014 Global top-down smoke-aerosol emissions estimation using satellite fire radiative power measurements *Atmos. Chem. Phys.* **14** 6643–67

Jaffe D A, O'Neill S M, Larkin N K, Holder A L, Peterson D L, Halofsky J E and Rappold A G 2020 Wildfire and prescribed burning impacts on air quality in the United States *J. Air Waste Manage. Assoc.* **70** 583–615

Jiang X, Wiedinmyer C and Carlton A G 2012 Aerosols from fires: an examination of the effects on ozone photochemistry in the Western United States *Environ. Sci. Technol.* **46** 11878–86

Kaiser J W *et al* 2011 Biomass burning emissions estimated with a global fire assimilation system based on observed fire radiative power *Biogeoscience* **9** 527–54

Keeley J E and Syphard A D 2019 Twenty-first century California, USA, wildfires: fuel-dominated vs. wind-dominated fires *Fire Ecol.* **15** 1–5

Key C H 2006 Ecological and sampling constraints on defining landscape fire severity *Fire Ecol.* **2** 34–59

Key C H and Benson N C 2006 Landscape assessment (LA) *FIREMON: Fire Effects Monitoring and Inventory System*

ed D Lutes *et al* (Fort Collins, CO: Department of Agriculture, Forest Service, Rocky Mountain Research Station) p 55 RMRS-GTR-164

Kolden C A, Lutz J A, Key C H, Kane J T and van Wagtendonk J W 2012 Mapped versus actual burned area within wildfire perimeters: characterizing the unburned *For. Ecol. Manage.* **286** 38–47

Kolden C A, Smith A M S and Abatzoglou J T 2015 Limitations and utilisation of Monitoring Trends in Burn Severity products for assessing wildfire severity in the USA *Int. J. Wildland Fire* **24** 1023–8

Larkin N K, Raffuse S M and Strand T M 2014 Wildland fire emissions, carbon, and climate: U.S. emissions inventories *For. Ecol. Manage.* **317** 61–69

Lindaas J *et al* 2020 Emissions of reactive nitrogen from Western U.S. wildfires during summer 2018 *J. Geophys. Res. Atmos.* **126** e2020JD032657

Liu T, Mickley L J, Marlier M E, DeFries R S, Khan M F, Latif M T and Karambelas A 2020 Diagnosing spatial biases and uncertainties in global fire emissions inventories: Indonesia as regional case study *Remote Sens. Environ.* **237** 111557

McLauchlan K K *et al* 2020 Fire as a fundamental ecological process: research advances and frontiers ed G Durigan *J. Ecol.* **108** 2047–69

Meng R and Zhao F 2017 Remote sensing of fire effects: a review for recent advances in burned area and burn severity mapping *Remote Sensing of Hydrometeorological Hazards* (Boca Raton, FL: CRC Press) pp 261–83

Miller J D and Thode A E 2007 Quantifying burn severity in a heterogeneous landscape with a relative version of the delta Normalized Burn Ratio (dNBR) *Remote Sens. Environ.* **109** 66–80

Parks S A 2014 Mapping day-of-burning with coarse-resolution satellite fire-detection data *Int. J. Wildland Fire* **23** 215–23

Parks S, Holsinger L, Voss M, Loehman R and Robinson N 2018 Mean composite fire severity metrics computed with Google Earth Engine offer improved accuracy and expanded mapping potential *Remote Sens.* **10** 879

Permar W *et al* 2021 Emissions of trace organic gases from Western U.S. wildfires based on WE-CAN aircraft measurements *J. Geophys. Res. Atmos.* **126** e2020JD033838

Perry D A, Hessburg P F, Skinner C N, Spies T A, Stephens S L, Taylor A H, Franklin J F, McComb B and Riegel G 2011 The ecology of mixed severity fire regimes in Washington, Oregon, and Northern California *For. Ecol. Manage.* **262** 703–17

Picotte J J 2019 Composite burn index (CBI) data for the conterminous US, collected between 1996 and 2018: U.S. Geological Survey Data Release (https://doi.org/ 10.5066/P91BH1BZ)

Picotte J J, Cansler C A, Kolden C A, Lutz J A, Key C, Benson N C and Robertson K M 2021 Determination of burn severity models ranging from regional to national scales for the conterminous United States *Remote Sens. Environ.* **263** 112569

Pouliot G, Pierce T, Benjey W, O'Neill S M and Ferguson S A 2020 Wildfire emission modeling: integrating bluesky and SMOKE *14th Annual Int. Emission Inventory Conf. 11-14*

Prichard S J, O'Neill S M, Eagle P, Andreu A G, Drye B, Dubowy J, Urbanski S and Strand T M 2020 Wildland fire emission factors in North America: synthesis of existing data, measurement needs and management applications *Int. J. Wildland Fire* **29** 132

R Core Team 2021 *R: A Language and Environment for Statistical Computing* (Vienna: R Foundation for Statistical Computing)

Raffuse S M, Larkin N K and Lahm P W 2012 Development of version 2 of the wildland fire portion of the National Emissions Inventory *20th Int. Emission Inventory Conf.*

Reid C E, Brauer M, Johnston F H, Jerrett M, Balmes J R and Elliott C T 2016 Critical review of health impacts of wildfire smoke exposure *Environ. Health Perspect.* **124** 1334–43

Reinhardt E D, Keane R E and Brown J K 1997 *First order fire effects model: FOFEM 4.0, user's guide* (No. 344-345) (US Department of Agriculture Forest Service Intermountain Research Station)

Rollins M G 2009 LANDFIRE: a nationally consistent vegetation, wildland fire, and fuel assessment *Int. J. Wildland Fire* **18** 235–49

Stephens S L *et al* 2013 Temperate and boreal forest mega-fires: characteristics and challenges *Front. Ecol. Environ.* **12** 115–22

Thomas D, Butry D, Gilbert S, Webb D and Fung J 2017 *The Costs and Losses of Wildfires* NIST Special Publication 1215 (Gathersburg, Maryland, United States of America: National Institute of Standards and Technology) p 1215

Turner M G, Hargrove W W, Gardner R H and Romme W H 1994 Effects of fire on landscape heterogeneity in Yellowstone National Park, Wyoming *J. Veg. Sci.* **5** 731–42

Val Martin M, Heald C L, Ford B, Prenni A J and Wiedinmyer C 2013 A decadal satellite analysis of the origins and impacts of smoke in Colorado *Atmos. Chem. Phys.* **13** 7429–39

van der Werf G R *et al* 2017 Global fire emissions estimates during 1997–2016 *Earth Syst. Sci. Data* **9** 697–720

van der Werf G R, Randerson J T, Collatz G J, Giglio L, Kasibhatla P S, Arellano A F, Olsen S C and Kasischke E S 2004 Continental-Scale Partitioning of Fire Emissions During the 1997–2001 El Niño/La Niña Period *Science* **303** 73–76

van der Werf G R, Randerson J T, Giglio L, Collatz G J, Kasibhatla P S and Arellano A F 2006 Interannual variability in global biomass burning emissions from 1997 to 2004 *Atmos. Chem. Phys.* **6** 3423–41

van der Werf G R, Randerson J T, Giglio L, Collatz G J, Mu M, Kasibhatla P S, Morton D C, DeFries R S, Jin Y and van Leeuwen T T 2010 Global fire emissions and the contribution of deforestation, savanna, forest, agricultural, and peat fires (1997–2009) *Atmos. Chem. Phys.* **10** 11707–35

Westerling A L 2016 Increasing Western US forest wildfire activity: sensitivity to changes in the timing of spring *Phil. Trans. R. Soc.* B **371** 20150178

Wiedinmyer C, Akagi S K, Emmons L K, Al-Saadi J A, Orlando J J, Soja A J and Soja A J 2011 The Fire INventory from NCAR (FINN): a high resolution global model to estimate the emissions from open burning *Geosci. Model Dev.* **4** 625–41

Williams A P, Abatzoglou J T, Gershunov A, Guzman-Morales J, Bishop D A, Balch J K and Lettenmaier D P 2019 Observed Impacts of Anthropogenic Climate Change on Wildfire in California *Earth's Future* **7** 892–910